frontiers | Frontiers in Geochemistry

TYPE Original Research
PUBLISHED 06 March 2025
DOI 10.3389/fgeoc.2025.1507366

OPEN ACCESS

EDITED BY
Jon Telling,
Newcastle University, United Kingdom

REVIEWED BY
Hualong Hong,
Xiamen University, China
James Lyons,
Planetary Science Institute, United States

*CORRESPONDENCE
Ian D. Bull,
ian.d.bull@bristol.ac.uk

RECEIVED 07 October 2024
ACCEPTED 14 January 2025
PUBLISHED 06 March 2025

CITATION
Reay MK, Simpson IA, Zhao W, Coningham RAE, Davis C, Acharya KP, Manuel M, Strickland K, Gilliland K, Kinnaird TC and Bull ID (2025) Triterpenoid wax esters confirm *Ficus religiosa* in archaeological sequences within the Mayadevi temple shrine, Lumbini – the birthplace of Buddha.
Front. Geochem. 3:1507366.
doi: 10.3389/fgeoc.2025.1507366

Triterpenoid wax esters confirm *Ficus religiosa* in archaeological sequences within the Mayadevi temple shrine, Lumbini – the birthplace of Buddha

Michaela K. Reay[1], Ian A. Simpson[2], Wanyue Zhao[1], Robin A. E. Coningham[2], Christopher Davis[2], Kosh Prasad Acharya[3], Mark Manuel[2], Keir Strickland[4], Krista Gilliland[5], Tim C. Kinnaird[6] and Ian D. Bull[1]*

[1]Organic Geochemistry Unit, School of Chemistry, University of Bristol, Bristol, United Kingdom, [2]Department of Archaeology, Durham University, Durham, United Kingdom, [3]Department of Archaeology, Government of Nepal, Kathmandu, Nepal, [4]Department of Archaeology and History, La Trobe University, Melbourne, VIC, Australia, [5]Western Heritage, Edmonton, AB, Canada, [6]School of Earth and Environmental Sciences, University of St Andrews, Scotland, United Kingdom

Leaf wax biomarkers permit chemotaxonomic identification of past vegetation in archaeological contexts. At the birthplace of Buddha, Lumbini in Nepal, archaeological evidence of a multi-phase tree shrine from the earliest beginnings of Buddhism has been uncovered in archaeological sequences within the Mayadevi Temple. As yet there has been no scientific attempt to establish the species of tree(s) occupying the "central open space" within the ancient shrine, or in the wider sacred landscape, despite this being an issue of significance for understanding early Buddhist practice. The cuticular leaf waxes of three tree species sacred and venerated in Buddhist tradition - *Saraca asoca*, *F. religiosa* and *Shorea robusta* were characterised, with additional identification achieved following hydrolysis of triterpenoid esters. Diagnostic distributions of triterpenoid esters were observed for *F. religiosa* leaves (β-amyrin, α-amyrin and lupeol esters with $C_{16:0}$, $C_{18:2}$, $C_{18:1}$, $C_{18:0}$, $C_{20:2}$, $C_{20:1}$, $C_{20:0}$, and $C_{22:0}$ fatty acids, Ψ-taraxasteryl eicosanoate, Ψ-taraxasterol behenate) and *S. robusta* leaves (taraxeryl linoleate). Chronologically controlled and contextualised analyses of archaeological soil lipids characterise the triterpenoid ester distribution within the main shrine's "central open space", an adjacent palaeo-channel, the monastic site and early village mound. The presence of β-amyrin palmitate and α-amyrin palmitate, with longer-chain homologues (β-amyrin stearate, α-amyrin stearate and β-amyrin eicosadienoate) in the soil indicate that the *F. religiosa* tree occupied the "central open space" throughout development of the tree shrine, alongside a *F. religiosa* grove close to the palaeo-channel adjacent to the Mayadevi Temple. Beyond these locations, *F. religiosa* occurred only rarely in the historic Lumbini landscape, although there are enhanced triterpenoid esters in a foundation pit in the village and in an occupation surface from the monastic site; there is no biomarker evidence of other trees. *F. religiosa* is a sacred tree species

of long-standing in South Asia; our analysis indicates its transition into Buddhist religious culture and demonstrates that leaf-wax biomarkers can provide enhanced visibility to archaeological tree shrines in South Asia.

KEYWORDS

biomarker, triterpenoid, soil, Buddha, Lumbini, ficis religiosa, leaf wax, lipid

Introduction

Leaf waxes predominantly comprise hydrocarbons, alkanols, and wax (alkyl/triterpenyl) esters. These non-polar molecules, with characteristic long alkyl chains, are generally found on the outer surface of plants (Harwood and Russell, 1984). Individual plants have characteristic lipid distributions within the cuticular wax, enabling differentiation from one another (Eigenbrode and Espelie, 1995). Leaf waxes are deposited into soil following leaf senescence and fall, their hydrophobicity conferring a degree of recalcitrance. Even if the carbon skeleton is modified, it can still be assigned to an original precursor (Maxwell et al., 1971). Furthermore, a high degree of hydrophobicity results in reduced loss through water leaching (Lloyd et al., 2012). These attributes make leaf waxes potentially diagnostic in archaeological settings as they are less likely to be lost from soils over time (Evershed, 1993). Their preservation over geological time means that they are widely used to reconstruct temperature and vegetation compositions in the sedimentary archive (Eglinton and Eglinton, 2008). Compositional differences in leaf waxes between plant species permits chemotaxonomic identification of previous vegetation cover based on one (Sonibare et al., 2005; Bossard et al., 2013) or multiple (Zhang et al., 2006; Lemma et al., 2019; Weber and Schwark, 2020) classes of leaf waxes. Distributions of *n*-alkanes and *n*-alkanols have been applied to reconstruct past vegetation, while triterpenoids and triterpenoid esters can be used as specific biomarkers for vegetation in the sedimentary and archaeological record (e.g., Dudd and Evershed, 1999; Oyo-Ita et al., 2010; Bossard et al., 2013; Courel et al., 2019). Hence, characterisation of soil lipid distributions in archaeological settings can reveal changes to overlying vegetation in antiquity and provide indicators that may inform on ancient ritual and religious practice.

Tree shrines, or *bodhigaras*, are a feature of many contemporary Buddhist temples, particularly in Sri Lanka and South East Asia, and there are hundreds of ancient representations in coinage and sculpture as well as descriptions in ancient texts (Coningham et al., 2013). Their popular use both signifies the association of trees within key events in the life of the historic, Gautama Buddha, such as his birth and enlightenment, as well as him physically through aniconic means (Nugteren, 2005). The birthplace of Gautama Buddha, Lumbini in Nepal's western Terai region, comprises the remains of shrines, monasteries and stupas set around two key monuments, the Mayadevi Temple, and a sandstone pillar recording the personal pilgrimage to this holy site by the Mauryan Emperor Asoka (r. 274-232 BCE). Initial archaeological excavations in the 1990s ascribed the oldest brick structure at the site to the reign of Asoka (Uesaka, 2001; JBF, 2005). However, later excavations found this monument had been superimposed on two earlier structures, both defining the same "central open space," the later with a paved platform around a substantial brick-kerb, chronometrically dated to between 400 and 200 BCE, and the earliest represented by linear wooden post-holes, dated to the 6th century BCE (Coningham et al., 2013; Coningham and Milou, 2001; 2022a; 2022b). Field stratigraphy and associated micromorphology analyses indicated that this "space" had been open to the elements and occupied by a tree, or trees (Coningham et al., 2013). This has been interpreted as a rare systematically excavated archaeological example of a South Asian tree shrine, changing structurally over some 300 years while maintaining the constancy of the tree in the "central space" (Coningham et al., 2013). With the alignment between chronologies and traditions associated with the birth of the Buddha, born to Queen Mayadevi at Lumbini around the middle of the first millennium BCE as she grasped a tree, it was suggested that the archaeological evidence at Lumbini represents identification of the "earliest Buddhist shrine" (Coningham et al., 2013), a view shared by other commentators (Fogelin, 2015).

However, to-date, support for the occurrence of a tree, or trees, in the "central open space" at the Mayadevi Temple has relied on field stratigraphy characterisation of root channels, micromorphological analyses of the channel fills and surfaces together with the depiction of tree shrines in early historical architectural reliefs (Cunningham, 1879; Bidari, 1996; Sponsel and Natadecha-Sponsel, 2003; Coningham et al., 2013). Earlier excavation of the Asokan structure identified charcoal derived from tree roots, with their stratigraphic context considered to be beneath the temple foundation footings rather than a tree shrine "central open space." Subsequent scanning electron microscope (SEM) analyses of charcoal fragments identified the species as *Shorea robusta* (JBF, 2005). However, questions remain as to what species of tree occupied the tree shrine "central open space" as the Mayadevi Temple developed structurally.

Non-lipid biomarkers have previously been applied to determine the distribution and ritual importance of cacao (*Theobroma cacao* L.) groves in ancient Mesoamerica (Terry et al., 2022). However, lipid biomarkers have yet to be applied to investigate the historic presence of sacred tree species in South Asia, especially at major religious sites, with the application of leaf wax biomarker analyses of archaeological stratigraphies having the potential to offer new and direct insight of tree species presence at the Mayadevi Temple and its associated archaeological landscape, as well as at other religious sites. There are three tree species associated with the Lord Buddha and sacred to Buddhism: *Saraca asoca*, *F. religiosa* and *S. robusta*. *S. asoca* is thought to be the tree under which the Lord Buddha was born, although alternative trees are also mentioned in Buddhist literatures including *F. religiosa* and *S. robusta*. *F. religiosa* is universally agreed as the tree under which the Lord Buddha attained

enlightenment with this species having a long pre-Buddhist tradition as a sacred tree species in the Indus Civilisation in the third millennium BCE (Marshall, 1931). *S. robusta* is traditionally the tree beneath which the Lord Buddha passed away and is the dominant species in forest areas of the Terai around Lumbini (Bidari, 1996; Nugteren, 2005; Tiwari et al., 2021).

Here, apolar lipid profiles for fresh leaves from *S. asoca*, *F. religiosa* and *S. robusta* growing today in the Lumbini Development Trust garden area, and found in the surrounding landscape, were characterised to identify specific biomarkers for the three sacred tree species. We subsequently analysed selected soil stratigraphies from the temple "central open space" together with soil from the surrounding archaeological landscape to determine if sacred tree species were present, based on preserved biomarkers. These analyses aim to provide new insights to the appearance and religious practices associated with the early Buddhist shrines within the Mayadevi Temple sequence. Furthermore, the methods and results have the potential to underpin new efforts to assess the presence and abundance of sacred tree species in Lumbini and in archaeological landscapes throughout South Asia.

Materials and methods

Site and stratigraphic contexts

Sampling of leaves and archaeological soils for sacred-tree species leaf-wax analyses was undertaken within the UNESCO Lumbini World Heritage Site property and its immediate buffer zone (N27 28 8.004 E83 16 33.996). The site is located at *ca*.150 m above sea level in the Rupandehi District of the alluvial Terai region of Nepal. The Terai is characterised by a range of alluvial deposits originating in the Himalaya and includes mega-fans, sheet wash, alluvial ridge deposition related to palaeo-channel floodplains and lake deposits; the past 100,000 years of these geomorphic processes are represented in the upper 50 m of sediment stratigraphy (Upreti, 1999; Verardi, 2007; Guillot et al., 2015; Sigdel and Sakai, 2016; Dingle et al., 2020). Minor and seasonal rivers with lower peak discharges originating in the Siwalik to the north of Lumbini also contribute to the local geomorphology by creating local fans and alluvial ridges in inter-fluvial locations. Local geomorphic influences at Lumbini include the incised Telar, Ghoraha and Harahawa rivers with annual discharges of *ca*. 160 m^3 s^{-1}, although now reduced by water drawn for irrigation (Suwal and Bhuju, 2006). Soils formed in the alluvial features of the Terai are typically deep, loamy textured and stone free. They are classified as Eutric Gleysols (FAO World Resource Base) having base saturations ≥50% together with reductimorphic and oximorphic colour patterns reflecting wetting and drying (Carson et al., 1985; Lamichhane et al., 2021). Bank-full river discharge and extensive flooding occurs during the monsoon season. The climate is sub-tropical, with an average annual temperature of 25°C and rainfall of 1200–3000 mm y^{-1}, mostly falling in the monsoon period (June-September) with a currently decreasing rainfall trend (Pokharel and Hallett, 2015; Sah et al., 2021). *S. robusta* is dominant in the remaining, and often conserved, forested areas. *F. religiosa* and *S. asoca* are also widespread but less frequent and natural associations between the three species are limited (Webb and Sah, 2003; Kunwar and Bussmann, 2006; Timilsina et al., 2007). All three tree species are currently found within the Lumbini Development Trust area (Tiwari et al., 2021).

Leaves (n = 5) from the mature sacred tree species (*S. asoca, F. religiosa* and *S. robusta*) were collected from the Lumbini Development Trust garden area and transported fresh to the laboratory. Soil samples were collected from key contexts of four chronologically controlled archaeological stratigraphies in and immediately adjacent the Mayadevi Temple during 2012 excavations (Figure 1). These stratigraphies are from within the Mayadevi Temple itself (MDT-C5; n = 5), the historic Lumbini "village mound" (LVM; n = 6), the monastic area adjacent the temple (LMS; n = 3) and a sediment infilled palaeo-channel beside the temple (LPC; n = 3; Table 1).

A combination of accelerator mass spectrometry radiocarbon (AMS ^{14}C) measurement of charcoal and optically stimulated luminescence (OSL) measurement of soil samples from across the site gives chronological control on stratigraphies (sixty measurements – 30 AMS ^{14}C, 30 OSL – undertaken at the Scottish Universities Environment Research Centre (SUERC)). The fourteen dating determinations (6 ^{14}C, 8 OSL) related to contexts sampled for lipid analyses are given in Supplementary Table S1. Age-depth modelling for sample LPC L2: 6009 is based on OxCal v. 4.4.4 (Bronk Ramsay, 2021). Integration of thin section micromorphology, field OSL profiling, field texture assessments and element composition by field X-ray fluorescence (XRF) analyses enabled interpretation of stratigraphy formation processes. These analyses give chrono-stratigraphic context to the biomarker analyses, summarised in Table 1.

Reagents and standards

All solvents were HPLC grade [*n*-hexane, dichloromethane (DCM), acetone, isopropanol (IPA) and methanol; Rathburn UK]. The internal standard mixture contained *n*-tetratriacontane (30 μg mL^{-1}), 2-hexadeconol (30 μg mL^{-1}), nonadecanoic acid (30 μg mL^{-1}) and 10-nonadecanone (10 μg mL^{-1}) in DCM-IPA (2:1 *v*/*v*). 50 μL was added to leaf and soils prior to extraction. *N,O*-bis(trimethylsilyl)trifluoroacteamide (BSTFA), containing 1% trimethylchlorosilane (TMCS) was purchased from Sigma-Aldrich for derivatisation of functionalised compounds.

Ultrasonic extraction of tree leaves

Leaves from the three mature tree species, collected from the Lumbini Development Trust garden area, were dried and finely cut. Leaves (0.5 g) were extracted using ultrasonic extraction (15 min) into DCM-acetone (9:1 *v*/*v*, 10 mL). Following ultrasonication, solvent was transferred following centrifugation (3000 rpm, 10 min). This was repeated three times, solvent combined and dried under a gentle stream of N_2 at 40°C. All extractions were carried out in triplicate.

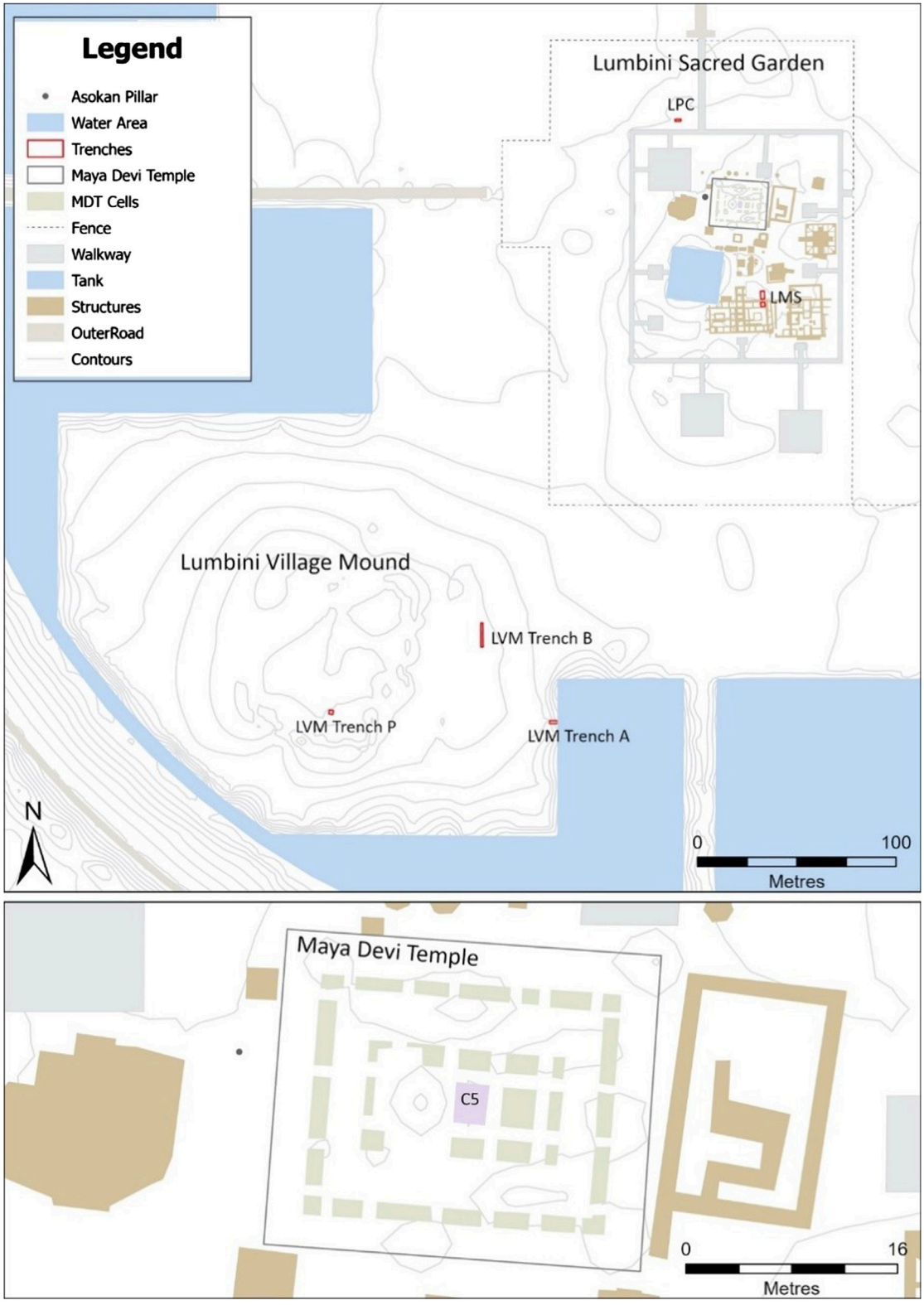

FIGURE 1
Lumbini Sacred Garden and Village Mound showing excavation trench locations.

TABLE 1 Biomarker samples: summary interpretations of chronological sequence and stratigraphic contexts. Supplementary Table S1 gives the AMS^{14}C and OSL measurements that are the basis for the Summary Chronology. See also Coningham et al. (2013) for further chronological sequencing.

Site	Lipid sample and stratigraphic context	Summary chronology	Context summary interpretation
Mayadevi Temple MDT (Trench C5)	L4: 513 (cuts through 507 and 508)	Mid 6thC - Mid 3rdC BCE	*"Tree root channel fill".* Evidenced by open microstructures, channel microstructures, recrystallised mineral material, cuts through linear context stratigraphic contexts
	L2: 508/517	Mid 6thC BCE	*"Tree shrine - central open space", raised surface, adjacent tree root channel fill.* Evidenced by contrasting mineralogy, textural pedofeatures, secondary calcite
	L3: 509 L1:509	Late 10thC BCE	*"Intensified agricultural landscape".* Evidenced by cultivation soil disturbance features, domestic refuse amendment, phytoliths, enhanced phosphorous signal
	L5: 510	Mid 15thC BCE Mid 13thC BCE	*"Agricultural landscape".* Evidenced by cultivation soil disturbance features, domestic refuse amendment, phytoliths
Lumbini Village Mound LVM (Trench P)	L6N: 1511/1518	Mid 10thC BCE	*"Surface within village, set beneath platform construction".* Compacted micro-structures, disturbance pedofeatures, occupational debris
	L3N: 1536, L5N: 1534 and L2E: 1538	Mid 13thC BCE	*"Shallow storage pits with post-abandonment fill".* Micro-sequences indicating preparation and lining of pits, fluvial micro-stratification and occupational wastes
	L4N: 1540/1532	Mid 36thC BCE	*"Natural fluvial deposits underlying village mound".* Sub-rounded and linear arrangements of coarse mineral material, vughy micropores, limpid clay coatings, Mg and Fe concretions
	L1E: 1524	Mid 7thC BCE (based on corresponding deep pit, Trench A)	*"Deep pits with cultural fill".* Traces of clay-based pit lining, Cultural fill dominated by ash (lower fill) and ceramics (upper fill). Currently interpreted as a foundation pit
Monastic Area LMS (Trench 1)	L1: 3017	Early 1stC CE	*Occupation surface:* Disturbed, occupational debris, fibrous organic material with compacted micro-horizon
	L2: 3030, L3: 3032	Mid 8thC - late 5thC BCE (based on corresponding Trench 2)	*Introduced laid material for monastery wall construction.* Dates reflect age of original deposit, mixed deposit, including exotic coarse mineral material (3032), compacted
Palaeo-channel LPC	L1: 6008	Early 5thC CE	*Fluvial deposits.* Particle size distribution, organic debris, clay weathering indicates very slow - stagnant river flow, seasonal movement of fine material reflected in textural pedofeatures, reduced iron
	L2: 6009	6thC BCE (based on age-depth modelling)	*Fluvial deposits.* Particle size distribution indicates slow river flow, seasonal movement of fine material reflected in textural pedofeatures, secondary iron movement
	L3: 6010	Late 8thC BCE	*Fluvial deposits.* Particle size distribution indicates slow river flow, seasonal movement of fine material reflected in textural pedofeatures, secondary iron movement

Soxhlet extraction of soils

Soils were lyophilised, finely ground and sieved (2 mm) to remove any vegetation or large stones. Sediment (30 g) was weighed into pre-extracted cellulose thimbles (DCM-acetone; 9:1 *v*/*v*, 6 h) and covered with furnaced (450°C, 4 h) glass wool. The sediments were Soxhlet extracted for 24 h with DCM-acetone (9:1, *v*/*v*). After extraction, the solvent was removed under reduced pressure to obtain a total lipid extract (TLE).

Acid/neutral separation of TLE

Dried TLEs from leaf and soil extractions were re-dissolved in DCM-IPA (1 mL, 2:1 *v*/*v*) and the acid and neutral fractions were separated using a solid phase extraction (SPE) cartridge with an aminopropyl bonded phase. The SPE cartridge was pre-eluted with 3% acetic acid in methanol (6 mL) and DCM-IPA (6 mL, 2:1 *v*/*v*). A neutral fraction was removed in DCM-IPA (6 mL, 2:1 *v*/*v*) and the acid fraction was eluted in 3% acetic acid in methanol (6 mL). All fractions were evaporated under a gentle stream of N_2 at 40°C.

Column chromatography of neutral lipids, derivatisation and instrument analyses

The neutral fraction dissolved in *n*-hexane (1 mL) was loaded onto the silica column, pre-eluted with hexane (6 mL). *n*-Hexane, DCM and DCM-methanol (1:1 *v*/*v*) were sequentially added to the column and eluted in a volume ratio of 2:3:2 to elute the

hydrocarbon, ketone/wax-ester and alcohol fractions, respectively. All fractions were dried under a gentle stream of N_2 at 40°C. The alcohol and ketone/wax ester fractions were derivatised with BSTFA +1%TMCS (30 µL) at 70°C for 1 h. Residual derivatising reagent was removed under a gentle stream of N_2 and fractions were re-dissolved in hexane prior to analysis.

Lipid fractions were analysed using a 7890 GC-FID (Agilent, Santa Clara, CA, United States) fitted with a DB-1HT (15 m × 0.32 mm i.d. × 0.1 µm film thickness; 100% dimethylpolysiloxane, Agilent). Injections (1 µL) were made using a 7683B autosampler *via* an on-column inlet. Helium was used as the carrier gas at a constant flow rate of 4.0 mL min^{-1}. The GC temperature program was as follows: 50°C (2 min) increased to 350°C (held for 20 min) at a rate of 10°C min^{-1}. The FID temperature was held at 350°C.

The lipid fractions were subsequently analysed by a 7890 GC coupled to a 7200B GC/Q-TOF MS (Agilent). Injections (1 µL) were made using a 7693 autosampler and an on-column inlet. The GC column and temperature were the same as for GC analyses. Helium was used as the carrier gas at a constant flow rate of 1.4 mL min^{-1}. The temperatures of the ion source, quadrupole and transfer line were set at 300°C, 180°C and 350°C, respectively. Data was acquired from *m/z* 50 to 1050 at a rate of 5 spectra s^{-1} using the Extended Dynamic Range mode. A standard mix consisting of palmitic acid, stearic acid, methyl heptadecanoate, methyl stearate, 1-palmitoyl-glycerol, cholesterol, tetratriacontane, dipalmitoyl-glycerol, trimyristate, cholesteryl oleate, tripalmitate, and tristearate was analysed (after trimethylsilylation) every 5 analytical runs to ensure chromatographic and mass spectrometric performance. Recovery of internal standards were all above 95% and limit of detection was 0.36 ng μL^{-1} for *n*-tetratriaconane, 0.47 ng μL^{-1} for 2-hexadecanol and 0.20 ng μL^{-1} for nonadecanone. GC/Q-TOF MS data were analysed using MassHunter Qual (Version B.07.00). Relative quantification was achieved using the internal standards, and ratios of determined biomarkers in comparison to the most abundant compound in the fraction. Confirmation that compounds in leaf waxes were present in sediments used a combination retention times and HRMS data.

Base hydrolysis of triterpenoid wax esters and instrument analyses

Initial analyses of the wax ester fraction from leaves indicated triterpenoid wax esters, which could not be unambiguously identified. Base hydrolysis of the wax ester fraction, to generate their constituent alcohol and *n*-alkanoic acid moieties, was used to support identifications. Identifications of triterpenoid wax esters are considered tentative due to the lack of available standards, although the use of multiple lines of evidence (i.e., combination of intact triterpenoid wax esters and hydrolysis, alongside elution orders) strongly supports the identifications presented herein. Ketone/wax ester fractions were dissolved in a 0.5 M methanolic solution of potassium hydroxide (2 mL) and heated at 80°C for 2 h. Hydrolysed mixtures were left to cool then acidified to pH 1 with 1.0 M hydrochloric acid solution and extracted with diethyl ether (2 × 1 mL). The organic extracts were combined and passed through an anhydrous sodium sulphate column to remove residual water. Diethyl ether was then evaporated under a gentle stream of N_2 at 40°C. Dried aliquots were derivatised with BSTFA +1%TMCS (30 µL) at 70°C for 1 h. Residual derivatising reagent was removed under at gentle stream of N_2 and fractions were re-dissolved in hexane prior to analysis.

Hydrolysed ketone/wax ester fractions were analysed using a Thermo Scientific ISQ7000 series GC-MS fitted with an HP1 column (50 m × 0.32 mm i.d. × 0.17 µm film thickness; 100% dimethylpolysiloxane, Agilent). The oven temperature program was as follows: 40°C (1 min) increased to 200°C at a rate of 10°C min^{-1}, followed by an increase to 300°C (held for 20 min) at a rate of 3°C min^{-1}. The GC was interfaced to the MS via a heated transfer line (300°C). The scan time was 0.2 s, the scan range was *m/z* 50-650, the ion source was held at 310°C and the ionisation mode was EI at 70 eV. Data acquisition and analysis used Xcalibur Version 4.1.31.9 (Thermo Fisher Scientific).

Results and discussion

Plant n-alkanes, n-alkanols and wax esters

The distributions of *n*-alkanes, *n*-alkanols and wax esters extracted from the reference leaf tissue of the sacred tree species are shown in Figure 2. *n*-Alkanes extracted from the *F. religiosa* leaves have carbon chain lengths ranging between C_{21} to C_{35}, where the predominant chain length is C_{27}. *n*-Alkanes extracted from the *S. robusta* leaf have chain lengths ranging between C_{25} to C_{35}, and the predominant chain length is C_{31}. A series of alkenes (C_{25}-C_{33}), with a maximum at C_{32}, is also observable in the alkane fraction from *S. robusta* leaves. *n*-Alkanes extracted from the *S. asoca* leaf have chain lengths ranging between C_{29} to C_{33} and the predominant chain length, is C_{31}. As expected, all leaves exhibited an odd-over-even predominance.

All leaves have an even-over-odd predominance for *n*-alkanols. The predominant *n*-alkanol homologues derived from the *F. religiosa* leaf have a chain length ranging from C_{24} to C_{34}. *n*-Alkanols derived from the *S. robusta* leaf have a chain length ranging from C_{28} to C_{34}, with only even chain lengths observed. *n*-Alkanols derived from the *S. asoca* leaf have a chain length ranging from C_{27} to C_{36}. Wax esters extracted from the *F. religiosa* leaf have a chain length range ranging from C_{42} to C_{54}, with an even-over-odd dominance. The predominant chain length was C_{46}. Wax esters extracted from the *S. robusta* leaf also have an even-over-odd dominance, with a most predominant chain length of C_{50} and a chain length ranging from C_{44} to C_{52}. Only even wax esters are observed in the *S. asoca* leaf, with a chain length between C_{46} to C_{54}. The most predominant chain length is C_{50}. Several sterols are also present in the alcohol fractions extracted from leaves. The relative distributions are shown in Supplementary Figure S1, with sitosterol the most dominant in *F. religiosa* and *S. asoca* leaves, with relatively higher amounts of other sterols and stanols (i.e., 5α-stigmastanol, campesterol, stigmasterol) identified in *F. religiosa* compared to *S. asoca* leaves. Stigmasterol is the most dominant sterol in *S. robusta* leaves. No free triterpenoids were observed.

Characteristic triterpenoid wax esters of religious trees

A series of compounds containing triterpenoid moieties were identified within the ketone/wax ester fraction of the sacred tree

10.3389/fgeoc.2025.1507366

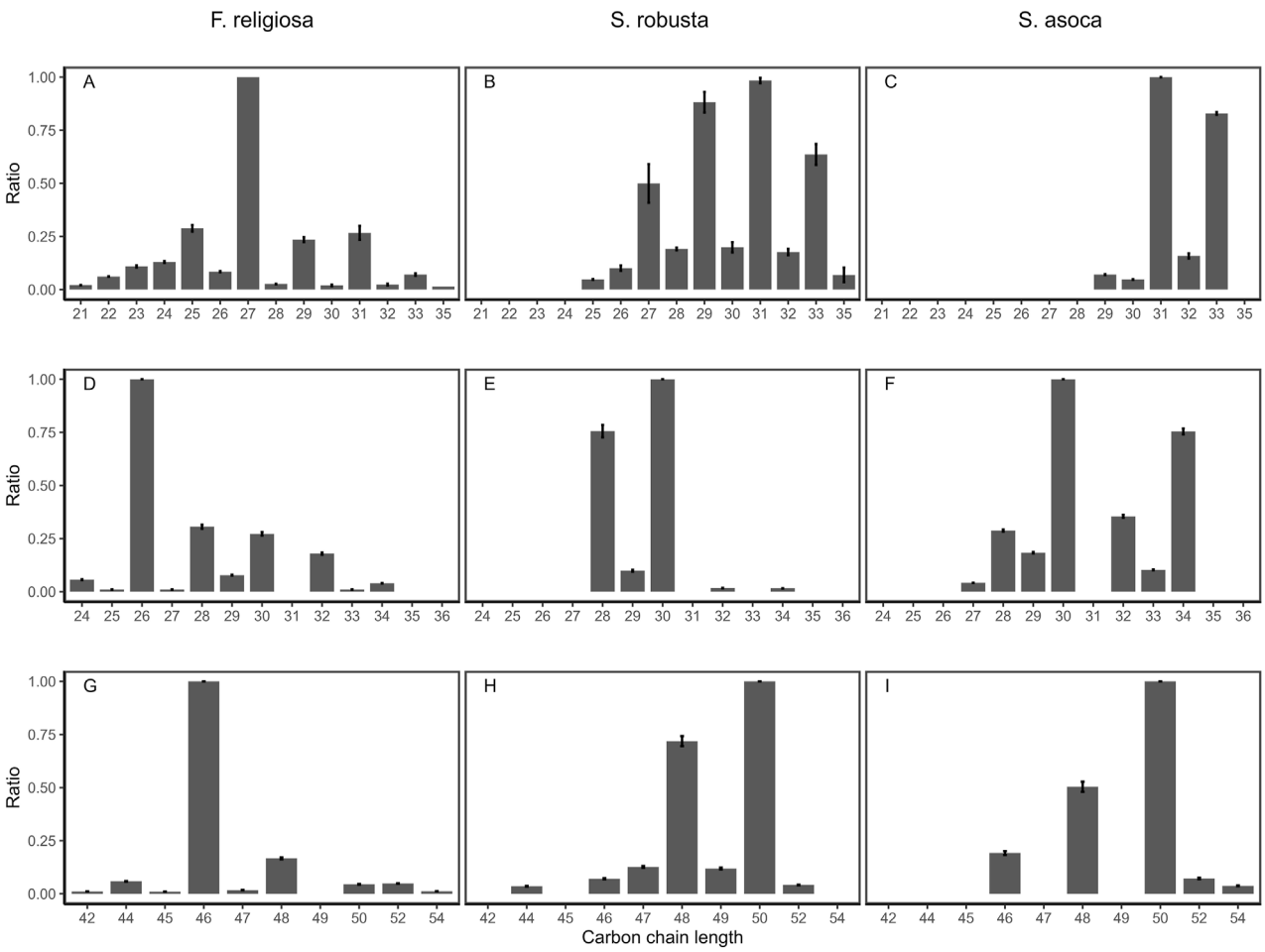

FIGURE 2
Carbon chain length distribution of *n*-alkanes **(A–C)**, *n*-alkanols **(D–F)** and wax esters **(G–I)** for the *F. religiosa*, *S. robusta* and *S. asoca* reference leaves.

species reference leaves, exhibiting the characteristic fragmentation of triterpenoids including a carbon-ring break and a retro Diels–Alder rearrangement (Djerassi et al., 1962; Budzikiewicz et al., 1963), yielding ions at *m/z* 218, 203/4, and 189. Triterpenoids are synthesised intracellularly, in the endoplasmic reticulum or cytoplasm via the mevalonate/acetate pathway to yield a C_{30} hydrocarbon (squalene) (Yan et al., 2014). This undergoes cyclisation to yield 3-deoxytripenes or 3-hydroxytriterpenes (Sawai and Saito, 2011), with additional functionalisation of the C skeleton to yield the huge variety [over 23,000 (Noushahi et al., 2022)], of triterpenoids observed in the natural environment. Triterpenoids have multiple roles in leaf waxes, including cuticle formation to help prevent water loss and protect against pests and pathogens, and acting as signalling molecules in plant growth and development (Tholl, 2015; Noushahi et al., 2022). The pentacyclic triterpenoids observed herein are in the form of esters, eluting within the latter part of the ketone/wax ester fraction, and which have previously been identified in leaf waxes [e.g., *Camellia sinensis* (Jetter and Sodhi, 2011; Zhou et al., 2019)]. The triterpenoid esters present in the leaves are shown in the Figure 3 partial ion chromatograms, and concentrations summarised in Table 2. The identifications were supported by base-catalysed hydrolysis of triterpenoid esters to yield the free triterpenoids (shown in Supplementary Material).

The *F. religiosa* leaf contains the largest range of triterpenoid esters, with 24 present (Figure 3A). Two early eluting triterpenoid wax esters (T^1 and T^2 in Figure 3A), which are also present in the *S. robusta* leaf are assigned as esters of β-amyrin and α-amyrin, respectively, although the chain length of the carboxylic acid moiety is unknown. The most abundant β-amyrin and α-amyrin triterpenoids are assigned as β-amyrin palmitate (T^4) and α-amyrin palmitate (T^5), which are only present in the *F. religiosa* leaves (β-amyrin palmitate:α-amyrin palmitate 0.59 for *m/z* 218). A number of triterpenoid wax esters where the ester chain length is C_{18} occur as a series of three in the *F. religiosa* leaves, comprising β-amyrin, α-amyrin and lupeol wax esters with linoleic acid ($C_{18:2}$; T^7, T^8, T^9, respectively), oleic acid ($C_{18:1}$; T^{10}, T^{11}, T^{12}, respectively) and stearic acid ($C_{18:0}$; T^{13}, T^{14}, T^{15}, respectively), all of which are also present as free fatty acids following hydrolysis (Supplementary Figure S2). The relative amounts of the unsaturated C_{18} fatty acid esters follow the trend β-amyrin > α-amyrin > lupeol esters, while lupeol stearate (T^{15}) is the most prevalent component of the $C_{18:0}$ series. Following hydrolysis, linolenic acid ($C_{18:3}$) is also observed (Supplementary

10.3389/fgeoc.2025.1507366

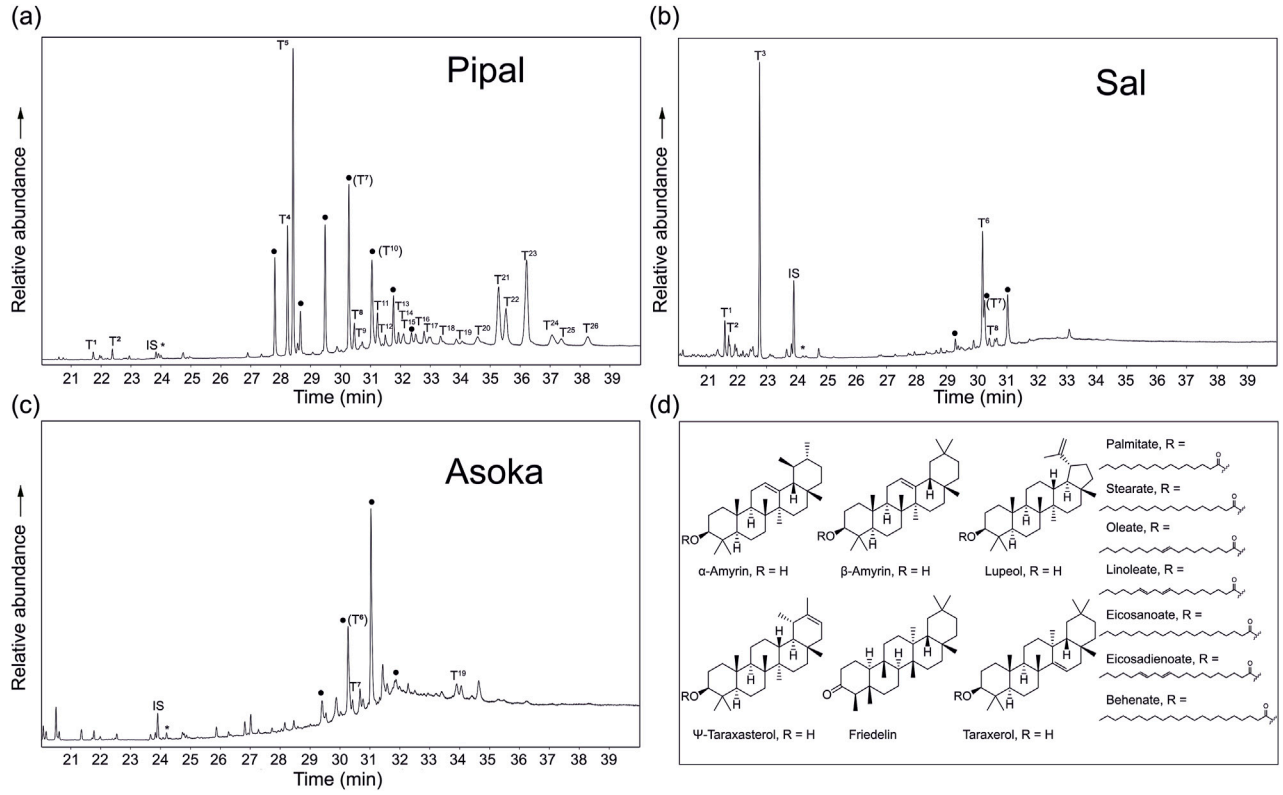

FIGURE 3
Partial total ion chromatograms of the ketone/wax ester fraction from **(A)** F. religiosa (Pipal) **(B)** S. robusta (Sala) and **(C)** S. robusta (Asoka) leaves containing wax esters and triterpenoid wax esters. Where T denotes triterpenoid esters (see Table 2 for identifications), ● denotes wax esters of carbon chain length C_{44} to C_{54}. IS denotes internal standard and * denotes contamination (plasticiser). **(D)** shows the structure of the triterpenoids and associated esters identified in the leaves.

Figure S2), however, this is not observed as a triterpenoid wax ester moiety, likely due to co-elution with $C_{18:1}$ and $C_{18:2}$ triterpenoid esters.

A similar series containing β-amyrin linoleate (T^7) and α-amyrin linoleate (T^8) is also observed in both the *S. robusta* (Figure 3B) and *S. asoca* (Figure 3C) leaves, while lupeol linoleate (T^9) is only observed in *F. religiosa* leaves. β-amyrin, α-amyrin and lupeol esters with eicosadienoic acid ($C_{20:2}$; T^{16}, T^{17}, T^{18}, respectively) are also assigned, while only β-amyrin, and lupeol esters with eicosenoic acid ($C_{20:1}$; T^{20}, T^{21}, respectively) are present. These fatty acids are not observed following hydrolysis (Supplementary Figure S2), however, the corresponding triterpenoid esters constitute a relatively low proportion, therefore, the fatty acids may be below detection limits. Relative retention times of the respective saturated triterpenoid wax esters for the components containing $C_{18:0}$ and $C_{20:0}$ moieties support this identification, with no odd carbon chain fatty acids observed to indicate triterpenoid wax esters with saturated or unsaturated C_{19} fatty acids. For $C_{20:0}$ and $C_{22:0}$ fatty acids, esters with β-amyrin (T^{21} and T^{24}, respectively), Ψ-taraxasterol (T^{22} and T^{25}, respectively) and lupeol (T^{23} and T^{26}, respectively) are identified, and relative amounts of the triterpenoids order as lupeol > β-amyrin > Ψ-taraxasterol. Two other triterpenoids are observed in the *S. robusta* leaves. Firstly, friedelin (T^3) is a cyclic terpene ketone which has been observed in plant species (Singh et al., 2023), and is the most prevalent triterpenoid in the *S. robusta* leaf. The second is identified as taraxeryl linoleate (T^6). Base hydrolysis confirms the taraxerol moiety of this triterpenoid ester, and elution prior to β-amyrin linoleate (T^7) and α-amyrin linoleate (T^8), as observed for the free triterpenoids, supports the assignment of the fatty acid moiety. The *S. asoca* leaves did not contain any additional triterpenoids which were not identified in the other leaves. The identified triterpenoid esters presented herein, particularly for *F. religiosa* and *S. robusta* leaves, provide a characteristic biomarker signature that can be used to identify locations where these tree species were present at Lumbini.

Biomarker identification in soils

Typical distributions of *n*-alkanes from soils at each location are shown in Supplementary Figure S3. For all soil contexts and locations, there is an odd-over-even predominance (range C_{21}-C_{39}) and the maximum chain length is C_{31} (Supplementary Figures S5, 6). There are two soil contexts which have a notably different distribution: LPC-12 1 and LMS-12 L3 (Supplementary Figures S4–6). The higher proportion of even homologues compared to the other soils may indicate an alternative source of alkanes (e.g., mineral wax). For the LPC soils, this likely reflects vegetation debris inputs to the palaeo-channel where preservation may have been

10.3389/fgeoc.2025.1507366

TABLE 2 Mass fraction of triterpenoids extracted from reference leaves (*F. religiosa, S. robusta and S. asoca*).

Triterpenoid number	Identification	Mass fraction/μg g^{-1}		
		F. religiosa	*S. robusta*	*S. asoca*
T^{1}	—	0.15 ± 0.03	0.74 ± 0.07	n.d
T^{2}	—	0.07 ± 0.01	0.42 ± 0.05	n.d
T^{3}	Friedelin	n.d	5.53 ± 0.45	n.d
T^{4}	β-amyrin palmitate	37.1 ± 2.6	n.d	n.d
T^{5}	α-amyrin palmitate	87.4 ± 4.8	n.d	n.d
T^{6}	Taraxeryl linoleate	n.d	2.20 ± 0.36	n.d
T^{7}	β-amyrin linoleate	49.8 ± 2.6	0.83 ± 0.10	0.50 ± 0.08
T^{8}	α-amyrin linoleate	7.83 ± 0.67	n.d	0.08 ± 0.01
T^{9}	Lupeol linoleate	2.55 ± 0.39	n.d	n.d
T^{10}	β-amyrin oleate	35.6 ± 2.7	n.d	n.d
T^{11}	α-amyrin oleate	12.6 ± 0.67	n.d	n.d
T^{12}	Lupeol oleate	3.95 ± 0.75	n.d	n.d
T^{13}	β-amyrin stearate	4.04 ± 0.40	n.d	n.d
T^{14}	α-amyrin stearate	4.75 ± 0.31	n.d	n.d
T^{15}	Lupeol stearate	3.33 ± 0.21	n.d	n.d
T^{16}	β-amyrin eicosadienoate	4.27 ± 0.24	n.d	n.d
T^{17}	α-amyrin eicosadienoate	3.17 ± 0.15	n.d	n.d
T^{18}	Lupeol eicosadienoate	5.32 ± 0.30	n.d	n.d
T^{19}	β-amyrin eicosaenoate	2.46 ± 0.27	n.d	1.03
T^{20}	Lupeol eicosaenoate	7.26 ± 0.65	n.d	n.d
T^{21}	β-amyrin eicosanoate	42.1 ± 1.3	n.d	n.d
T^{22}	Ψ-taraxasteryl eicosanoate	26.8 ± 1.1	n.d	n.d
T^{23}	Lupeol eicosanoate	65.4 ± 2.9	n.d	n.d
T^{24}	β-amyrin behenate	11.9 ± 1.1	n.d	n.d
T^{25}	Ψ-taraxasterol behenate	4.03 ± 0.51	n.d	n.d
T^{26}	Lupeol behenate	8.65 ± 0.49	n.d	n.d

All values are mean ± SE (n = 3) and n.d. indicates not detected.

greater compared to drier soil environments. However, comparison of these *n*-alkane distributions with *n*-alkane distributions isolated from the sacred tree species leaf reference material shows no correlating features to link a location with the occurrence of sacred tree species.

The alcohol fraction of the soils contains *n*-alkanols with some sterols also identified (Supplementary Figure S7). All soils exhibit an even-over-odd dominance, except LMS 12 L1 where no *n*-alkanols are observable. All soils have a similar distribution of *n*-alkanols (C_{20}-C_{32}), with a bimodal distribution and high amounts of the C_{22} and C_{32} homologues (Supplementary Figures S8, 9). The even-over-odd dominance, as observed for the leaf *n*-alkanols, confirms a general vegetative input to all locations due to synthesis of *n*-alkanols in leaves *via* reduction of fatty acids synthesised from acetate groups (Ohlrogge and Browse, 1995). However, this does not confirm the presence of sacred tree species in these locations, likely due to overprinting from other vegetation species. Furthermore, the presence of shorter-chain *n*-alkanols, not observed in the sacred tree species reference leaves, indicates other *n*-alkanol inputs and potential soil degradation of longer chain *n*-alkanols or esters.

Sterols were also identified in the archaeological soils (Supplementary Table S2). Sitosterol and 5α-stigmastanol were identified in 30% and 65% of soils, respectively. Campesterol was identified in LPC-12-L3, which also exhibits high amounts of other plant biomarkers, indicating relatively better preservation conditions, and/or a higher input from vegetation debris. The identified sterols and stanols all have plant sources and confirm the presence of plant-derived lipids but provide insufficient evidence to confirm the onetime occurrence of any sacred tree species at these locations. A series of monoacylglycerols (MAGs), diacylglycerols

10.3389/fgeoc.2025.1507366

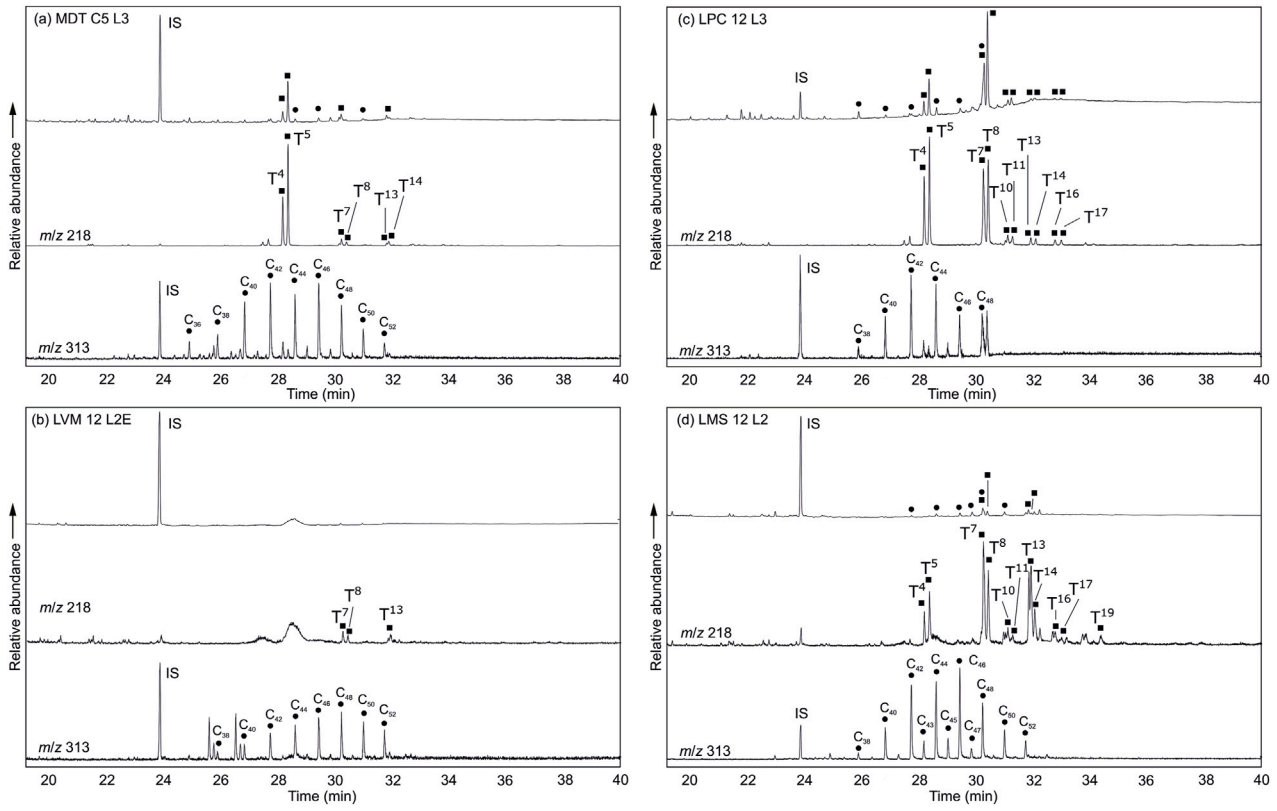

FIGURE 4
Typical partial ion chromatogram (TIC) and extracted ion chromatograms for triterpenoid esters (*m/z* 218) and wax esters (*m/z* 313) for four sites at Lumbini for **(A)** MDT C5 L3, **(B)** LVM 12 L2E, **(C)** LPC 12 L3 and **(D)** LMS 12 L2. IS denotes internal standard, C_n indicates wax ester chain length and triterpenoid ester numbering is from the sacred tree species reference leaves (Table 2).

(DAGs) and triacylglycerols (TAGs) were identified in all soils (Supplementary Table S2), although these are not observed in sacred tree species; both have plant and microbial sources (Alvarez and Steinbüchel, 2002; Xu and Shanklin, 2016). All soils exhibit distributions of wax esters (C_{34}-C_{54}) with an even-over-odd dominance (example chromatograms shown in Figure 4), and a maximum homologue ranging between C_{42} to C_{46} (Supplementary Figures S10, 11). All soils yield similar wax ester distributions but do not match the wax ester distributions observed for the sacred tree species. Furthermore, the presence of shorter chain wax esters indicates other sources of these compounds or *in-situ* processing of longer chain wax esters. As with the *n*-alkanes and *n*-alkanols, chain length analyses of wax esters are insufficient to confirm the presence of sacred tree species derived organic matter in the archaeological stratigraphies, although they do confirm the presence of vegetation in all areas. This likely results from overprinting from other species of vegetation which do not contain the *Ficus*-specific triterpenoid esters at this site. Overall, the evidence provided by *n*-alkanes, *n*-alkanols and wax esters confirm vegetation inputs, but are insufficient alone to confirm to a species level what may have been present across the history of Lumbini.

Triterpenoid esters identified in the plant reference material and in soils (Table 3) offer strong biomarker evidence for the presence of sacred tree species at Lumbini. In the Mayadevi temple stratigraphy (MDT), the triterpenoid esters identified in all soils are β-amyrin palmitate (T^4), α-amyrin palmitate (T^5), β-amyrin linoleate (T^7), α-amyrin linoleate (T^8) and β-amyrin stearate (T^{13}), with low amounts of other triterpenoid esters present [β-amyrin oleate (T^{10}; *n*=1), α-amyrin oleate (T^{11}; *n*=2), α-amyrin stearate (T^{14}; *n*=1), β-amyrin eicosadienoate (T^{16}; *n*=3), β-amyrin eicosaenoate (T^{21}; *n*=1); Table 3; Figure 4]. These triterpenoid esters are prevalent in the reference leaves, and the less prevalent lupeol esters are not observable in the archaeological soils. β-amyrin linoleate (T^7) and α-amyrin linoleate (T^8) are identified in all sacred tree species (Figure 3). However, ratios observed in the Mayadevi Temple soils are not consistent with ratios observed for leaves, therefore, the presence of β-amyrin linoleate (T^7) and α-amyrin linoleate (T^8) cannot be used to differentiate between tree species (Supplementary Figure S12). The diagnostic triterpenoid ester for *S. robusta* (taraxeryl linoleate T^6) is absent indicating this tree was likely not present in the area. There is not a *S. asoca* specific triterpenoid ester, and other biomarkers (e.g., *n*-alkanes, *n*-alkanols, wax esters) were not sufficiently specific to be able to determine the presence or absence of this tree. Therefore, whilst we cannot rule out that this tree was also present at the site, it cannot be determined using leaf waxes in soils. Other evidence would need to be explored to determine if this tree was present during the development of the tree shine at Lumbini, such as analysis of micro-remains (e.g., pollen, starch grains) or secondary metabolites (e.g., alkaloids) which may also be diagnostic to specific tree species.

TABLE 3 Summary of triterpenoids present in the soil locations (mass fraction ng g^{-1}). Triterpenoid numbering is taken from triterpenoids identified in reference leaves, in order of elution.

Site	Lipid sample and stratigraphic context	β-amyrin palmitate (T^4)	α-amyrin palmitate (T^5)	β-amyrin linoleate (T^7)	α-amyrin linoleate (T^8)	β-amyrin oleate (T^{10})	α-amyrin oleate (T^{11})	β-amyrin stearate (T^{13})	α-amyrin stearate (T^{14})	β-amyrin eicosadienoate (T^{16})	α-amyrin eicosadienoate (T^{17})	β-amyrin eicosaenoate (T^{19})
Mayadevi Temple MDT-C5	L4: 513	6.43	23.1	4.88	2.18			Tr				
	L2: 508/517	0.76	2.27	0.57	0.24			0.37		0.23		
	L3: 509	1.09	3.67	0.65	0.36			0.46				
	L1:509	2.03	7.33	0.55	1.45	Tr	Tr	Tr		Tr		Tr
	L5: 510	0.37	1.35	0.66	0.41		0.66	0.53	0.34			
Lumbini Village Mound LVM-12	L6N: 1518/1511	Tr	Tr	0.49	Tr			Tr				
	L3N: 1536	Tr	Tr	0.45	Tr			Tr				
	L5N: 1534	Tr	Tr	0.35	Tr			Tr				
	L2E: 1538	Tr	Tr	0.17	Tr			Tr				
	L4N: 1532/1540	Tr	Tr	Tr	Tr			Tr				
	L1E: 1524	0.19	0.37	0.60	Tr		Tr	Tr	Tr	Tr		
Monastic Area LMS-12	L1: 3017	1.47	3.87	1.65	2.41	0.56	0.38	Tr	Tr	Tr	Tr	
	L2: 3030	Tr	Tr	1.38	Tr	0.74	Tr	0.35	0.72	Tr	Tr	Tr
	L3: 3032	Tr	Tr									
Palaeo-channel LPC-12	L1: 6008	0.84	2.85	Tr	Tr	Tr	Tr	Tr	Tr	Tr	Tr	
	L2: 6009	1.77	8.18	0.93	Tr	0.37	Tr	0.42	Tr	0.49	Tr	
	L3: 6010	9.96	24.0	54.2	74.4	3.99	5.56	6.39	6.49	5.43	6.11	

Mass fractions are expressed in ng g^{-1} with Tr = Trace (very small mass fraction). Note T^1, T^2, friedelin (T^3), taraxeryl linoleate (T^6), lupeol linoleate (T^9), lupeol oleate (T^{12}), lupeol stearate (T^{15}), lupeol eicosadienoate (T^{18}), lupeol eicosaenoate (T^{20}), β-amyrin eicosanoate (T^{21}), Ψ-taraxasteryl eicosanoate (T^{22}), lupeol eicosanoate (T^{23}), β-amyrin behenate (T^{24}), Ψ-taraxasterol behenate (T^{25}) and lupeol behenate (T^{26}) were not present in the soils so are not included.

10.3389/fgeoc.2025.1507366

The presence of β-amyrin palmitate (T^4) and α-amyrin palmitate (T^5) throughout the Mayadevi Temple stratigraphy examined, which are identified only in the *F. religiosa* leaves, strongly supports the presence of this sacred tree species in the temple area. This is supported further by the relative amount of β-amyrin palmitate and α-amyrin palmitate (mean 0.57, *m*/*z* 218), correlating with observed ratios in *F. religiosa* reference leaves (0.59; *m*/*z* 218, Supplementary Figure S12), and the presence of β-amyrin stearate (T^{13}) and β-amyrin eicosadienoate (T^{16}) in the soils from the temple area, which are also only identified in *F. religiosa* leaves (Figure 3; Table 2). The highest amounts of β-amyrin palmitate (T^4) and α-amyrin palmitate (T^5) were identified in MDT-C5-L4, dating to the mid 6th to 3rd century BCE, concurrent with the 'central open space' of the early shrine. This, together with the stratigraphic and micro-stratigraphic evidence of root channels (Table 1), strongly indicates the existence of a tree shrine within the "central open space," specifically a *F. religiosa* tree(s). A second soil context, interpreted as a raised surface to create the "central open space" during the mid 6th century BCE, associated with the earliest wooden posthole tree shrine (Table 1), yields lower amounts of β-amyrin palmitate (T^4) and α-amyrin palmitate (T^5) still indicating the presence of *F. religiosa*. In pre-structural level soils from within the temple site sequences, β-amyrin palmitate and α-amyrin palmitate are also present. We suggest that, alongside the stratigraphic evidence of agricultural cultivation (Table 1), the triterpenoid ester analyses indicate that there was a grove of *F. religiosa* trees in this locality that predates the shrines. *F. religiosa*, both individually and grouped as groves, is recognised and well-understood as a ubiquitous and long-standing feature of South Asia religious life, and the biomarker evidence presented herein further supports its importance (During-Caspers and Nieskens, 1989; Parpola, 1992; Vergano, 2013; Thapa, 2015). While there is previous reported archaeological evidence of *S. robusta* in the temple (JBF, 2005), based on charcoal fragments, the presence of *S. robusta* is not supported by the biomarker evidence, due to the lack of taraxeryl linoleate (T^6) observed, the only specific triterpenoid ester for this sacred tree species. The absence of this triterpenoid ester suggests either that *S. robusta* was not present or was not the dominant species in the temple area and in the wider Lumbini landscape.

The palaeo-channel (LPC) adjacent to the temple site has relatively high amounts of the *F. religiosa* triterpenoid ester pair β-amyrin palmitate (T^4) and α-amyrin palmitate (T^5; Table 3; Figure 4). There were also several other triterpenoid esters identified [β-amyrin linoleate (T^7), α-amyrin linoleate (T^8), β-amyrin oleate (T^{10}), α-amyrin oleate (T^{11}), β-amyrin stearate (T^{13}), α-amyrin stearate (T^{14}), β-amyrin eicosadienoate (T^{16}), α-amyrin eicosadienoate (T^{17})] in this stratigraphy which are also present in the *F. religiosa* leaf. The β-amyrin:α-amyrin wax ester ratios were not consistent with the reference leaves, potentially due to post-deposition processing. The high amount of triterpenoid esters resulting from a greater quantity of vegetation debris entering the palaeo-channel following leaf senescence and fall supports the local presence of a *F. religiosa* grove, although this may also reflect more optimal anoxic preservation conditions in the river sediment. *F. religiosa* grew consistently in this locality, although with a reduced presence over time which may reflect local landscape pressures as the village and sacred area developed. *F. religiosa* trees prefer deep alluvial soils, consistent with the paleo-channel area (Upadhyay et al., 2019; Das et al., 2023). Stratigraphic and spatial contrasts in triterpenoid esters at Lumbini indicate that an early Buddhist tree shrine was created in or beside a *F. religiosa* grove adjacent to a slow-moving watercourse and on the periphery of the agricultural village landscape from the mid-6th century BCE.

One soil context from the monastery site (LMS 12 L1), dating from the early 1st century CE and interpreted as an occupation surface, also exhibited a triterpenoid ester distribution comparable to later phases of the paleo-channel, although the other soils from the monastery site only have trace levels of these triterpenoid esters present (Table 3; Figure 4). This suggests introduction of leaf debris to the monastery occupation surface and that the sacred significance of *F. religiosa* continued as the monastery developed. Very low trace amounts of triterpenoids [Table 3; β-amyrin palmitate (T^4), α-amyrin palmitate (T^5), α-amyrin linoleate (T^8) and β-amyrin stearate (T^{13})] with a higher amount of β-amyrin linoleate (T^7), are observed in all soils at the village mound (LVM; Table 2). These very low levels of triterpenoid esters in the pre-village mound context as well as in the village mound stratigraphy suggests a low number of *F. religiosa* trees in the immediate area of the village prior, although oxic soil conditions may also have increased degradation in this setting. An exception to the general trace levels of *F. religiosa* triterpenoid esters observed in this locality is the mid 7th century BCE deep pit with cultural fill, currently interpreted as a foundation pit (LVM-L1E; Table 3). This opens the possibility that as well as the ordered deposition of ceramics and ash in foundation pits, *F. religiosa* was also deliberately deposited, reflecting the ubiquitous significance of this species in pre-existing ritual behaviours and its overlap into Buddhist practice.

Conclusion

Analysis of leaf waxes has identified triterpenoid esters as diagnostic of sacred tree species growing at Lumbini, with other biomarkers (*n*-alkanes, *n*-alkanols, sterols, stanols and wax esters) only sufficient to indicate terrestrial vegetation. More specific biomarkers (triterpenoid wax esters) instead provide the strongest evidence of previous vegetation inputs in the archaeological context studied here. Triterpenoid esters within the archaeological soils confirm the presence of *F. religiosa* at Lumbini due to the presence of triterpenoid esters found only in this leaf at this site [β-amyrin palmitate (T^4), α-amyrin palmitate (T^5) and corresponding ratio)]. There is no evidence to support the presence of *S. robusta* as the specific triterpenoid ester (taraxeryl linoleate; T^6) for this tree was not identified in the archaeological soils, while there is no triterpenoid ester specific for *S. asoca.*

The spatial and temporal distribution of the triterpenoid esters specific to *F. religiosa* sheds new light onto the evolution of tree shrines through the development of the Mayadevi Temple site. Pre-dated by a grove of *F. religiosa* in an agricultural–village landscape prior to construction of the shrines, *F. religiosa* is subsequently evident in the presence of a tree shrine in the "central open space" from the mid 6th century BCE. Contemporary *F. religiosa* growth in the adjacent palaeo-channel stratigraphic sequence also indicates *F. religiosa* growth in this locality at the mid 6th century BCE, at the

time of shrine creation. In the wider Lumbini landscape, low levels of specific triterpenoid esters indicate lower amounts of *F. religiosa* leaf detritus. However, there are specific stratigraphies where high levels of the specific *F. religiosa* triterpenoid esters suggest the importance of this tree in both the Buddhist monastic community (1st century CE) and wider village culture (7th century BCE). These biomarker-based findings–with a focus on triterpenoid esters–give new archaeological visibility and significance to *F. religiosa* in its occurrence and perception within natural, agricultural–village and sacred historical landscapes. This work emphasises the importance of this species in the emergence of the sacred landscape at Lumbini. It also points towards a new science-based approach that can enhance the archaeological visibilities of tree shrines across South Asia.

Data availability statement

The original contributions presented in the study are included in the article/Supplementary Material, further inquiries can be directed to the corresponding author.

Author contributions

MR: Formal Analysis, Investigation, Methodology, Validation, Visualization, Writing–original draft, Writing–review and editing. IS: Conceptualization, Formal Analysis, Investigation, Resources, Visualization, Writing–original draft, Writing–review and editing. WZ: Formal Analysis, Investigation, Methodology, Visualization, Writing–review and editing. RC: Writing–review and editing. CD: Writing–review and editing. KA: Writing–review and editing. MM: Writing–review and editing. KS: Writing–review and editing. KG: Writing–review and editing. TK: Writing–review and editing. IB: Conceptualization, Formal Analysis, Funding acquisition, Investigation, Project administration, Resources, Supervision, Writing–original draft, Writing–review and editing.

Funding

The author(s) declare that financial support was received for the research, authorship, and/or publication of this article. The authors wish to thank the NERC for partial funding of the National Environmental Isotope Facility (NEIF; Contract No. NE/V003917/1), and for funding GC-MS capabilities via the 2014 Strategic Environmental Science Capital Call (Award No. CC010) to facilitate biomarker analyses.

Acknowledgments

We are extremely grateful to the Japanese-Funds-in-Trust-for-UNESCO, Lumbini Development Trust, Department of Archaeology (Government of Nepal) and UNESCO's Kathmandu Field Office for their support at Lumbini. We thank Helen L. Whelton for analytical assistance, and Katherine Hyland for sediment preparation.

Conflict of interest

The authors declare that the research was conducted in the absence of any commercial or financial relationships that could be construed as a potential conflict of interest.

The author(s) declared that they were an editorial board member of Frontiers, at the time of submission. This had no impact on the peer review process and the final decision.

Generative AI statement

The author(s) declare that no Generative AI was used in the creation of this manuscript.

Publisher's note

Supplementary material

The Supplementary Material for this article can be found online at: https://www.frontiersin.org/articles/10.3389/fgeoc.2025.1507366/full#supplementary-material

References

Alvarez, H., and Steinbüchel, A. (2002). Triacylglycerols in prokaryotic microorganisms. *Appl. Microbiol. Biotechnol.* 60, 367–376. doi:10.1007/s00253-002-1135-0

Bidari, B. (1996). Forest and trees associated with Lord Buddha. *Anc. Nepal* 139, 1124.

Bossard, N., Jacob, J., Le Milbeau, C., Sauze, J., Terwilliger, V., Poissonnier, B., et al. (2013). Distribution of miliacin (olean-18-en-3β-ol methyl ether) and related compounds in broomcorn millet (Panicum miliaceum) and other reputed sources: implications for the use of sedimentary miliacin as a tracer of millet. *Org. Geochem.* 63, 48–55. doi:10.1016/j.orggeochem.2013.07.012

Bronk Ramsay, C. (2021). OxCal v4.4.4. Available at: https://c14.arch.ox.ac.uk/oxcal.html.

Budzikiewicz, H., Wilson, J. M., and Djerassi, C. (1963). Mass spectrometry in structural and stereochemical problems. XXXII. Pentacyclic triterpenes. *J. Am. Chem. Soc.* 85, 3688–3699. doi:10.1021/ja00905a036

Carson, B., Shah, P., and Maharjan, P. (1985). Land resource mapping Project (LRMP). *Land Syst. Rep. Soil Landscapes Nepal.*

Coningham, R. A. E., Acharya, K. P., Strickland, K. M., Davis, C. E., Manuel, M. J., Simpson, I. A., et al. (2013). The earliest Buddhist shrine: excavating the birthplace of the Buddha, Lumbini (Nepal). *Antiquity* 87, 1104–1123. doi:10.1017/S0003598X00049899

Coningham, R. A. E., and Milou, J.-F. (2001). Reactive monitoring mission to Lumbini, birthplace of Lord Buddha: report and recommendations of a UNESCO mission to Nepal. *Kathmandu.*

Coningham, R. A. E., and Milou, J.-F. (2022a). Reflections on a report for the 2001 international technical meeting for the conservation, presentation and development of maya devi temple remains, Lumbini World heritage site, Nepal. *Anc. Nepal* 211, 33–47.

Coningham, R. A. E., and Milou, J.-F. (2022b). Reflections on the 2000 UNESCO reactive monitoring mission to Lumbini, birthplace of Lord Buddha. *Anc. Nepal* 211, 5–32.

Courel, B., Adam, P., and Schaeffer, P. (2019). The potential of triterpenoids as chemotaxonomic tools to identify and differentiate genuine, adulterated and archaeological balsams. *Microchem. J.* 147, 411–421. doi:10.1016/j.microc.2019.03.035

Cunningham, A. (1879). in *The stupa of bharhut*. Editor W. H. Allen (London).

Das, A., Gujre, N., Devi, R. J., Rangan, L., and Mitra, S. (2023). "Traditional ecological knowledge towards natural resource management: perspectives and challenges in North East India," in *Sustainable agriculture and the environment*. Editors M. Farooq, N. Gogou, and M. Pisante (Academic Press), 275–294.

Dingle, E. H., Creed, M. J., Sinclair, H. D., Gautam, D., Gourmelen, N., Borthwick, A. G. L., et al. (2020). Dynamic flood topographies in the Terai region of Nepal. *Earth Surf. Process. Landforms* 45, 3092–3102. doi:10.1002/esp.4953

Djerassi, C., Budzikiewicz, H., and Wilson, J. M. (1962). Mass spectrometry in structural and stereochemical problems unsaturated pentacyclic triterpenoids. *Tetrahedron Lett.* 3, 263–270. doi:10.1016/S0040-4039(00)70864-1

Dudd, S. N., and Evershed, R. P. (1999). Unusual triterpenoid fatty acyl ester components of archaeological birch bark tars. *Tetrahedron Lett.* 40, 359–362. doi:10.1016/S0040-4039(98)02311-9

During-Caspers, E. C. L., and Nieskens, P. J. M. (1989). "The 'calendar stone' from mohenjo-daro reconsidered," in *South asian Archaeology 1989*. Editors C. Jarrige, J. P. Gerry, and R. H. Meadow (Madison: Prehistory Press), 83–95.

Eglinton, T. I., and Eglinton, G. (2008). Molecular proxies for paleoclimatology. *Earth Planet. Sci. Lett.* 275, 1–16. doi:10.1016/j.epsl.2008.07.012

Eigenbrode, S. D., and Espelie, K. E. (1995). Effects of plant epicuticular lipids on insect herbivores. *Annu. Rev. Entomol.* 40, 171–194. doi:10.1146/annurev.en.40.010195.001131

Evershed, R. P. (1993). Biomolecular archaeology and lipids. *World Archaeol.* 25, 74–93. doi:10.1080/00438243.1993.9980229

Fogelin, L. (2015). *An archaeological history of Indian buddhism*. Oxford University Press. doi:10.1093/acprof:oso/9780199948215.001.0001

Guillot, S., Garçon, M., Weinman, B., Gajurel, A., Tisserand, D., France-Lanord, C., et al. (2015). Origin of arsenic in late pleistocene to holocene sediments in the nawalparasi district (Terai, Nepal). *Environ. Earth Sci.* 74, 2571–2593. doi:10.1007/s12665-015-4277-y

Harwood, J. L., and Russell, N. J. (1984). *Lipids in plants and microbes*. Netherlands: Springer. doi:10.1007/978-94-011-5989-0

JBF (2005). Lumbini: the archaeological survey report 1992-1995. Tokyo.

Jetter, R., and Sodhi, R. (2011). Chemical composition and microstructure of waxy plant surfaces: triterpenoids and fatty acid derivatives on leaves of *Kalanchoe daigremontiana*. *Surf. Interface Analysis* 43, 326–330. doi:10.1002/sia.3430

Kunwar, R. M., and Bussmann, R. W. (2006). Ficus species in Nepal: a Review. *Lyonia* 11, 85–97.

Lamichhane, S., Kumar, L., and Adhikari, K. (2021). Updating the national soil map of Nepal through digital soil mapping. *Geoderma* 394, 115041. doi:10.1016/j.geoderma.2021.115041

Lemma, B., Mekonnen, B., Glaser, B., Zech, W., Nemomissa, S., Bekele, T., et al. (2019). Chemotaxonomic patterns of vegetation and soils along altitudinal transects of the Bale Mountains, Ethiopia, and implications for paleovegetation reconstructions – Part II: lignin-derived phenols and leaf-wax-derived *n*-alkanes. *E&G Quat. Sci. J.* 68, 189–200. doi:10.5194/egqsj-68-189-2019

Lloyd, C. E. M., Michaelides, K., Chadwick, D. R., Dungait, J. A. J., and Evershed, R. P. (2012). Tracing the flow-driven vertical transport of livestock-derived organic matter through soil using biomarkers. *Org. Geochem.* 43, 56–66. doi:10.1016/j.orggeochem.2011.11.001

Marshall, J. H. (1931). *Mohenjo-daro and the Indus civilization*. London: Arthur Probsthain.

Maxwell, J. R., Pillinger, C. T., and Eglinton, G. (1971). Organic geochemistry. *Q. Rev. Chem. Soc.* 25, 571. doi:10.1039/qr9712500571

Noushahi, H. A., Khan, A. H., Noushahi, U. F., Hussain, M., Javed, T., Zafar, M., et al. (2022). Biosynthetic pathways of triterpenoids and strategies to improve their Biosynthetic Efficiency. *Plant Growth Regul.* 97, 439–454. doi:10.1007/s10725-022-00818-9

Nugteren, A. (2005) "Belief, bounty and beauty: rituals around sacred trees in India," in *NUMEN book series studies in the history of religions; No. 108*. Leiden: Brill.

Ohlrogge, J., and Browse, J. (1995). Lipid biosynthesis. *Plant Cell.* 7, 957–970. doi:10.1105/tpc.7.7.957

Oyo-Ita, O. E., Ekpo, B. O., Oros, D. R., and Simoneit, B. R. T. (2010). Occurrence and sources of triterpenoid methyl ethers and acetates in sediments of the cross-river system, southeast Nigeria. *Int. J. Anal. Chem.* 2010, 1–8. doi:10.1155/2010/502076

Parpola, A. (1992). "The 'fig deity seal' from mohenjo-daro: its iconography and inscription," in *South asian Archaeology 1989*. Editors C. Jarrige, J. P. Gerry, and R. H. Meadow (Madison: Prehistory Press), 227–236.

Pokharel, A. K., and Hallett, J. (2015). Distribution of rainfall intensity during the summer monsoon season over Kathmandu, Nepal. *Weather* 70, 257–261. doi:10.1002/wea.2544

Sah, S., Singh, R., Chaturvedi, G., and Das, B. (2021). Trends, variability, and teleconnections of long-term rainfall in the Terai region of India. *Theor. Appl. Climatol.* 143, 291–307. doi:10.1007/s00704-020-03421-y

Sawai, S., and Saito, K. (2011). Triterpenoid biosynthesis and engineering in plants. *Front. Plant Sci.* 2, 25. doi:10.3389/fpls.2011.00025

Sigdel, A., and Sakai, T. (2016). Sedimentary facies analysis of the fluvial systems in the Siwalik Group, Karnali River section, Nepal Himalaya, and their significance for understanding the paleoclimate and Himalayan tectonics. *J. Nepal Geol. Soc.* 51, 11–26. doi:10.3126/jngs.v51i0.24084

Singh, S. K., Shrivastava, S., Mishra, A. K., Kumar, D., Pandey, V. K., Srivastava, P., et al. (2023). Friedelin: structure, biosynthesis, extraction, and its potential health impact. *Molecules* 28, 7760. doi:10.3390/molecules28237760

Sonibare, M. A., Jayeola, A. A., and Egunyomi, A. (2005). Chemotaxonomic significance of leaf alkanes in species of Ficus (Moraceae). *Biochem. Syst. Ecol.* 33, 79–86. doi:10.1016/j.bse.2004.05.010

Sponsel, L. E., and Natadecha-Sponsel, P. (2003). "Buddhist views of nature and the environment," in *Nature across cultures. Science across cultures: the history of non-western science*. Editor H. Selin (Dordrecht: Springer), 351–371.

Suwal, R., and Bhuju, U. (2006). "Lumbini: an environmental analysis," in *UNESCO Office in Kathmandu," in* Lumbini: Present status and future challenges, 89–101.

Terry, R. E., Brown, B. M., Stanton, T. W., Ardren, T., Anaya, T. C., Lowry, J., et al. (2022). Soil biomarkers of cacao tree cultivation in the sacred cacao groves of the northern Maya lowlands. *J. Archaeol. Sci. Rep.* 41, 103331. doi:10.1016/j.jasrep.2021.103331

Thapa, C. B. (2015). Some socio-religious flora of Rupandehi district, western Nepal. *Int. J. Appl. Sci. Biotechnol.* 3, 123–126. doi:10.3126/ijasbt.v3i1.12217

Tholl, D. (2015). "Biosynthesis and biological functions of terpenoids in plants," in *Biotechnology of isoprenoids*. Editors J. Schrader, and J. Bohlmannm (Springer), 63–106.

Timilsina, N., Ross, M. S., and Heinen, J. T. (2007). A community analysis of sal (Shorea robusta) forests in the western Terai of Nepal. *For. Ecol. Manag.* 241, 223–234. doi:10.1016/j.foreco.2007.01.012

Tiwari, A., Tiwari, P., and Pathak, M. L. (2021). Plant diversity in Lumbini Area: plants related to Guatam Buddha's life need ecological restoration. *J. Plant Resour.* 19, 7597.

Uesaka, S. (2001). *Archaeological research at maya devi temple*. Tokyo: Lumbini.

Upadhyay, K. K., Japang, B., Singh, N. S., and Tripathi, S. K. (2019). Status and socio-ecological dimensions of sacred groves in Northeast India. *J. Appl. Nat. Sci.* 11, 590–595. doi:10.31018/jans.v11i3.2121

Upreti, B. N. (1999). An overview of the stratigraphy and tectonics of the Nepal Himalaya. *J. Asian Earth Sci.* 17, 577–606. doi:10.1016/S1367-9120(99)00047-4

Verardi, G. (2007). *Excavations at gotihawa and pipri, kapilbastu District, Nepal*. Rome.

Vergano, D. (2013). Oldest Buddhist shrine uncovered in Nepal may push back the Buddha's birth date. *Natl. Geogr.*

Webb, E. L., and Sah, R. N. (2003). Structure and diversity of natural and managed sal (Shorea robusta Gaertn.f.) forest in the Terai of Nepal. *For. Ecol. Manag.* 176, 337–353. doi:10.1016/S0378-1127(02)00272-4

Weber, J., and Schwark, L. (2020). Epicuticular wax lipid composition of endemic European Betula species in a simulated ontogenetic/diagenetic continuum and its application to chemotaxonomy and paleobotany. *Sci. Total Environ.* 730, 138324. doi:10.1016/j.scitotenv.2020.138324

Xu, C., and Shanklin, J. (2016). Triacylglycerol metabolism, function, and accumulation in plant vegetative tissues. *Annu. Rev. Plant Biol.* 67, 179–206. doi:10.1146/annurev-arplant-043015-111641

Yan, X.-J., Gong, L.-H., Zheng, F.-Y., Cheng, K.-J., Chen, Z.-S., and Shi, Z. (2014). Triterpenoids as reversal agents for anticancer drug resistance treatment. *Drug Discov. Today* 19, 482–488. doi:10.1016/j.drudis.2013.07.018

Zhang, Z., Zhao, M., Eglinton, G., Lu, H., and Huang, C. (2006). Leaf wax lipids as paleovegetational and paleoenvironmental proxies for the Chinese Loess Plateau over the last 170kyr. *Quat. Sci. Rev.* 25, 575–594. doi:10.1016/j.quascirev.2005.03.009

Zhou, X., Chen, X., Du, Z., Zhang, Y., Zhang, W., Kong, X., et al. (2019). Terpenoid Esters are the major constituents from leaf lipid droplets of Camellia sinensis. *Front. Plant Sci.* 10, 179. doi:10.3389/fpls.2019.00179